Aerosol and Air Quality Research, 13: 1423–1437, 2013

ISSN: 1680-8584 print / 2071-1409 online
doi: 10.4209/aaqr.2012.11.0306

Numerical Simulation of Ultrafine Particle Dispersion in Urban Street Canyons with the Spalart-Allmaras Turbulence Model

Mauro Scungio[1*], Fausto Arpino[1], Luca Stabile[1], Giorgio Buonanno[1,2]

[1] *Department of Civil and Mechanical Engineering, University of Cassino and Southern Lazio, via G. di Biasio 43, 03043 Cassino (FR), Italy*
[2] *Queensland University of Technology, GPO Box 2434, Brisbane Qld, 4001, Australia*

ABSTRACT

The increased traffic emissions and reduced ventilation of urban street canyons lead to the formation of high particle concentrations as a function of the related flow field and geometry. In this context, the use of advanced modelling tools, able to evaluate particle concentration under different traffic and meteorological conditions, may be helpful.

In this work, a numerical scheme based on the non-commercial fully explicit AC-CBS algorithm, and the one-equation Spalart-Allmaras turbulence model, was developed to perform numerical simulations of fluid flow and ultrafine particle dispersion in different street canyon configurations and under different wind speed and traffic conditions. The proposed non-commercial numerical tool was validated through a comparison with data drawn from the scientific literature.

The results obtained from ultrafine particle concentration simulations show that as the building height increases the dispersion of particles in the canyon becomes weaker, due to the restricted interaction between the flow field in the street canyon and the undisturbed flow. Higher values of approaching wind speed facilitate the dispersion of the particles. The traffic effect has been evaluated by imposing different values of particles emission, depending on the vehicles type, with the lowest concentration values obtained for the Euro 6 vehicles, and the highest for High Duty Vehicles. A parametric analysis was also performed concerning the exposure to particles of pedestrians in different positions at the road level as a function of street canyon geometry, traffic mode, and wind speed. The worst exposure (1.25×10^6 part./cm^3) was found at the leeward side for an aspect ratio $H/W = 1$, wind speed of 5 m/s when High Duty Vehicles traffic was considered.

Keywords: Street canyon; Turbulence; Modelling; Ultrafine particles.

INTRODUCTION

Ultrafine Particles in Urban Areas

Management of urban air quality is a key aspect in reducing the personal exposure to typical traffic-related pollutants and their resulting health effects. Among these pollutants, in the last decades ultrafine particles (UFPs, particle smaller than 100 nm in diameter) are receiving particular attention as they are recognized to cause adverse health effects (Pope and Dockery, 2006).

Monitoring atmospheric aerosol is important for several reasons: the toxic nature of the particles due to the organic compounds on itself (Eiguren-Fernandez *et al.*, 2010), the ability of UFPs to penetrate in the epithelial cells of the lower respiratory tract and accumulate in lymph nodes (Nel *et al.*, 2006), the oxidative damage effects on DNA which may increase the risk of cancer (Møller *et al.*, 2008), and the potential association with paediatric asthma (Andersen *et al.*, 2008) are some of the harmful effects on human health caused by exposure to nanoparticles.

Vehicular traffic is considered the main contributor to UFPs emission (Kittelson *et al.*, 2004; Gidhagen *et al.*, 2005) even if a threshold limit value for emission from light passenger and commercial vehicles has been stated in terms of particle number (Commission Regulation (EC) No. 692/2008); such local source, along with the development of clusters of buildings and the increasing vehicular traffic, are some of the reasons for deterioration of air quality in urban areas. This is the case of the so called street canyon, which is a typical urban configuration of a street flanked by buildings on both sides. In a street canyon, air exchange provided by natural ventilation may become weak with consequent formation of high particle concentration zones. For these reasons, urban microenvironments may increase human short-term exposure to high particle concentrations, and significantly contribute to the increase of the daily dose (Buonanno *et al.*, 2011; Buonanno *et al.*, 2012), leading to worsening of existing pulmonary and cardiovascular disease

* Corresponding author.
Tel.: +39-0776-2993618
E-mail address: m.scungio@unicas.it

(Pope III and Dockery, 2006; Brugge *et al.*, 2007; Andersen *et al.*, 2010).

From a legislative point of view, air quality threshold limit values are only stated in terms of particle mass: PM_{10} (particulate matter collected by a selective inlet with a 50% cut-off efficiency at 10 μm of aerodynamic diameter) and $PM_{2.5}$ (particulate matter collected by a selective inlet with a 50% cut-off efficiency at 2.5 μm of aerodynamic diameter). In particular, the European Directive (Directive 2008/50/EC) provides a limit concentration value of 50 $\mu g/m^3$ on daily basis for PM_{10}, and guidelines for $PM_{2.5}$. Such limit has been stated only in terms of average values and does not take into account daily variations of particle concentration which could be related to atmospheric dynamic or source emission characteristics. Moreover, only an amount of fixed sampling points (FSPs) are recommended by EU Directive 99/30 (Council Directive 1999/30/EC) for monitoring of air quality in urban areas as a function of the citizen number, adopting these values for the entire population living nearby, without analysing the orographic and microclimatic characteristics of the site. This approach completely neglects UFP monitoring, so becoming too simplified for the understanding of the real human exposure to pollutants since individuals move through multiple urban microenvironments that may affect their daily and long-term exposure to airborne particles. The real exposure is influenced by several parameters including street geometry, road layout, vehicle emissions, meteorological conditions and driving and walking behaviours which can influence the aerosol dynamic (Briggs *et al.*, 2008; Buonanno *et al.*, 2011).

Numerical Modelling of UFPs Distribution Inside Street Canyons

Measurement in FSPs cannot be properly used to characterize the real human exposure to airborne particles in micro-environments such as street canyons. This experimental approach to evaluate particle concentration levels in urban areas is inadequate for several reasons: the number of sampling points is scanty; the choice of the sampling point position is influenced by practical constraints; and the measurements are only representative of the micro-climatic and traffic conditions taking place during the sampling period. The complexity of the analysed phenomena makes Computational Fluid Dynamics (CFD) models a promising tool to evaluate particle concentration levels in every point of the micro-environment under consideration, by solving the mass, momentum, turbulence and pollutant dispersion equations.

Since the dispersion of pollutants is strongly influenced by the turbulent flow field established in the canyon, a suitable turbulence model is needed. Amongst different turbulence modelling approaches, Reynolds Averaged Navier-Stokes (RANS) based models are widely used in simulations of flow and pollutant dispersion when the geometrical layout is complex (Venetsanos *et al.*, 2003; Kim and Baik, 2004; Xie *et al.*, 2005). The most commonly used model for the simulation of turbulent flows in street canyons is the well-known two equations k-ε model (Launder and Spalding, 1974). Other models use a single transport equation for the evaluation of eddy viscosity, requiring less computational resource. In some recent works, the LES (Large Eddy Simulation) technique was adopted (Walton and Cheng, 2002; Liu *et al.*, 2004; Liu *et al.*, 2005; Letzel *et al.*, 2008). According to LES approach, large eddies are resolved directly by the computational grid while the effects of the small, unresolved eddies are modelled. However, LES technique is very computationally demanding (Walton and Cheng, 2002). In addition, even though the LES technique is able to provide information about instantaneous fluctuations of concentration field, which cannot be obtained by RANS computations, more detailed investigations are required for its application in street canyons (Tominaga and Stathopoulos, 2011). In this paper, the RANS approach and the one equation Spalart-Allmaras (SA) turbulence model (Spalart and Allmaras, 1992) are employed. The use of the one equation SA model, allows to save computational resources when complex three-dimensional domains are considered and also offers the possibility to switch to a Detached Eddy Simulation (DES) scheme. The DES option attempts to combine the best features of RANS and LES (Viswanathan and Tafti, 2006; Hasse *et al.*, 2009; Paik *et al.*, 2009), and represents a future development of this work. Such a hybrid approach reduces to RANS near solid boundaries and to LES away from the wall and is very promising for fully three-dimensional studies of pollutants dispersion modelling in urban areas.

Several models addressing dispersion of gaseous pollutants and particulate matter (on a mass basis) at different urban scales are currently available. These may include simple box models, Lagrangian or Eulerian models, Gaussian models and Computational Fluid Dynamics (CFD) based models (Sharma and Khare, 2001; Vardoulakis *et al.*, 2003; Holmes and Morawska, 2006; Li *et al.*, 2006).

Referring to UFPs dispersion, very few models able to specifically take into account the UFPs dynamics are nowadays available to predict particle number concentrations inside street canyons. Vignati *et al.* (1999) used a modal particle transformation model, coupled to a jet plume diffusion model, to estimate the coagulation and particle growth due to water uptake. In their study, they demonstrated that coagulation was insignificant due to the rapid dilution of the fresh emitted particles. Using the same jet plume model coupled to a monodisperse dynamical aerosol model, Pohjola *et al.* (2003) also showed that coagulation is of negligible importance in street environments. In this work, the coagulation-condensation processes were neglected, since in outdoor environments dilution typically prevails over the growth of the particles, as reported from Ketzel and Berkowicz (2004). The dilution was taken into account by properly setting the size of the domain where particle emission is imposed.

In a future development of the model, the simulation will be extended to polidisperse aerosols, moreover, the coagulation-condensation processes will be taken into account.

Aims of the Work

In this work, numerical modelling of UFPs dispersion in

street canyons is performed using the RANS type Spalart-Allmaras one equation turbulence model and a *K*-theory dispersion model (Moreira and Vilhena, 2010). These models are solved through a non-commercial fully explicit algorithm: the Artificial Compressibility (AC)-Characteristic Based Split (CBS) scheme (Massarotti *et al.*, 2006; Arpino *et al.*, 2010). The use of a fully explicit algorithm involves a matrix inversion free procedure that offers several advantages, such as low computing requirements even for complex three-dimensional problems and the possibility of simple and efficient parallelization. The required robustness of the algorithm has been obtained developing a stability analysis based on the order of magnitude of each term of the governing equations, while the proposed model has been validated by comparing the obtained results with reference data available in the scientific literature (Arpino *et al.*, 2011). The use of a non-commercial numerical tool offers the required flexibility when complex phenomena coupled to each other need to be modelled, over and above the possibility of directly handling the code, virtually eliminating any limitation deriving from the use a commercial CFD software.

The performance of the proposed AC-CBS algorithm, in conjunction to the SA turbulence model and the *K*-theory dispersion model, has been firstly assessed by simulating a wind tunnel study of car exhaust dispersion in street canyon, available in the scientific literature (Meroney *et al.*, 1996). A mixture of ethane and air was used to simulate the dispersion of pollutant in the street canyon model, thus the AC-CBS algorithm was set to simulate the dispersion of such gas, defining appropriate Neumann type boundary condition and diffusion coefficient for the specie under investigation. Then, the validated model was applied to the simulation of UFPs dispersion in different street canyon configurations. The diffusion coefficient used in the simulation is a function of the particle size under examination.

The validation of the SA turbulence model in the AC-CBS scheme here adopted, has been reported in a previous work of the authors (Arpino *et al.*, 2011) and represents the first step of the development of a complete pollution dispersion model in a three-dimensional urban area.

MATERIALS AND METHODS

Governing Equations of the Turbulent Flow Field

Since the wind direction is assumed perpendicular to the street canyon, a two-dimensional computational domain was considered in the simulations. The air inside the street canyon was assumed to be incompressible with constant density and kinematic viscosity. As the proposed model is at its first stage of development, thermal effects have not been taken into account. Kim and Baik (2001) and Sini *et al.* (1996) have shown that thermal effects inside urban street canyons may influence both fluid flow patterns and pollutant dispersion. Thermal effects will be included in future developments of the model. For brevity, only an outline of the mathematical model will be given here, while a more detailed description may be found in scientific literature (Brooks and Hughes 1982; Zienkiewicz *et al.*, 2005). The dimensionless conservation of mass and momentum equations are:

Mean-continuity:

$$\frac{1}{\beta^2}\frac{\partial \overline{p}}{\partial t}+\frac{\partial\left(\overline{u}_i\right)}{\partial x_i}=0 \tag{1}$$

Mean-momentum:

$$\frac{\partial \overline{u}_i}{\partial t}+\frac{\partial}{\partial x_j}\left(\overline{u}_j\overline{u}_i\right)=-\frac{\partial \overline{p}}{\partial x_i}+\frac{\partial\left(\tau_{ij}+\tau_{ij}^R\right)}{\partial x_j} \tag{2}$$

where $\overline{u}_i$ denotes the averaged velocity component in the *i*-direction, $\overline{p}$ the averaged pressure field, τ_{ij} is the laminar shear stress tensor, and β is an artificial compressibility parameter. The Reynolds-stress tensor τ_{ij}^R is introduced to relate the nonlinear term $\overline{u}_j'\overline{u}_i'$, with the averaged variables, according to the Boussinesq hypothesis:

$$\tau_{ij}^R=-\overline{u}_i'\overline{u}_j'=\frac{\nu_T}{\mathrm{Re}}\left(\frac{\partial \overline{u}_i}{\partial x_j}+\frac{\partial \overline{u}_j}{\partial x_i}-\frac{2}{3}\frac{\partial \overline{u}_k}{\partial x_k}\delta_{ij}\right)-\frac{2}{3}\kappa\delta_{ij} \tag{3}$$

In the Eq. (3), the turbulent kinetic energy, κ, is often dropped for simplicity (Zienkiewicz *et al.*, 2005). The eddy viscosity ν_T is computed via an intermediate variable $\hat{\nu}$ through the relation:

$$\nu_T=\hat{\nu}f_{v1}\left(\chi\right) \tag{4}$$

The intermediate variable $\hat{\nu}$ is computed by solving the SA turbulence model, based on the following non-dimensional transport equation:

$$\frac{\partial \hat{\nu}}{\partial t}+\frac{\partial\left(\overline{u}_j\hat{\nu}\right)}{\partial x_j}=c_{b1}\hat{S}\hat{\nu}+\frac{1}{\mathrm{Re}\,\sigma}\left[\frac{\partial}{\partial x_i}\left\{\left(1+\hat{\nu}\right)\frac{\partial \hat{\nu}}{\partial x_i}\right\}+c_{b2}\left(\frac{\partial \hat{\nu}}{\partial x_i}\right)^2\right]-\frac{c_{w1}f_w}{\mathrm{Re}}\left[\frac{\hat{\nu}}{y}\right]^2 \tag{5}$$

Further details about terms and constants of the SA model can be found in the scientific literature (Spalart and Allmaras, 1992) and are not reported here for brevity.

Stability Conditions

The present AC-CBS algorithm is based on a fully explicit time iterative procedure. Therefore, an accurate stability analysis is required for the calculation of appropriate time step limits at each pseudo-temporal iteration (D'Acunto, 2004; Hirsch, 2007; Arpino *et al.*, 2008). A stabilization procedure, based on an order of magnitude analysis of each term in the conservation equations, has been recently developed and successfully applied to the AC-CBS algorithm, also in the presence in very large source terms. Details about such procedure can be found in Arpino *et al.* (2010) and

Arpino *et al.* (2009), and are not provided here for brevity.

Species Transport Equation

In order to calculate the pollutant dispersion, an Eulerian approach based on a *K*-closure model was used (Moreira and Vilhena, 2010). Such models are most suited to deal with complex problems, such as the dispersion of pollutants over complex terrain or the diffusion of non-inert pollutants, and are based on the numerical resolution of the following mass conservation equation of the chemical species, written invoking the Boussinesq hypothesis:

$$\frac{\partial \overline{c}}{\partial t} + \overline{u} \cdot \nabla \overline{c} = \left(D + \nu_T \right) \nabla^2 \overline{c} + \overline{S} \tag{6}$$

where $\overline{c}$ is the averaged concentration and ν_T the eddy viscosity, D and $\overline{S}$ are the molecular diffusion coefficient and the emission strength of the chemical specie, respectively.

Stability Conditions for the Species Transport Equation

The species conservation equation is explicitly solved within the numerical procedure and a stability analysis is required to ensure the needed robustness. On the basis of the order of magnitude analysis approach, adopted for the stabilization of fluid flow equations, a stability condition in terms of pseudo time-step limitation has been derived for each term of the species transport equation:

Convective term

$$\Delta t_{conv} \le \frac{h}{\overline{u}^n_{conv}} \tag{7}$$

Diffusive term

$$\Delta t_{diff} \le \frac{h^2}{2D + \nu_T} \tag{8}$$

Source term

$$\Delta t_{source} \le \frac{\overline{c}}{S} \tag{9}$$

where h is the mesh element size, computed as the minimum of the ratio between the element area and the element side length at the opposite of each node; $\overline{c}$ is the concentration and S is the source strength value. The nodal optimum time-step adopted in the simulation is the minimum value obtained from the application of relations (7)–(9).

AC-CBS Scheme

The AC-CBS algorithm is based on the temporal discretization along the characteristics of the flow. The spatial discretization is obtained by employing the standard Galerkin finite element procedure (Brooks and Hughes 1982; Zienkiewicz *et al.*, 2005). The AC-CBS method combines the operator splitting with the standard artificial compressibility procedure to obtain a stable solution.

The scheme is essentially based on three steps: in the first step, an intermediate velocity field is calculated; in the second step, the pressure is obtained from the resolution of the continuity equation; and, in the third step, the intermediate velocity field is corrected to get the final velocity values. Further steps can be added as a function of the problem under investigation. In this work the scalar equation of the SA turbulence model and the species conservation equation are solved as a fourth and fifth step of the algorithm, respectively. Further details about the AC-CBS algorithm can be found in (Massarotti *et al.*, 2006; Arpino *et al.*, 2010; Arpino *et al.*, 2011).

Model Validation Case: Tracing Gas Dispersion in an Isolated Street Canyon Model

To assess the performance of the present AC-CBS scheme in the calculation of turbulent fluid flow and pollutant dispersion, the wind tunnel study of car exhaust dispersion in street canyon achieved by Meroney *et al.* (1996) was reproduced. This experimental study was performed in the atmospheric boundary layer wind tunnel (BLASIUS) of the Meteorological Institute of Hamburg University, obtaining vertical profiles of pollutant concentration in several points of the "in scale" street canyon, for different values of the approaching wind velocity. A Mixture of ethane and air was used to simulate the dispersion of pollutants; the continuous linear pollutant source was experimentally approximated by a line of closely spaced point sources, located at the bottom of the canyon in the centre of the street floor.

Computational Domain for the Model Validation Case

In Fig. 1 the street canyon configuration reproduced for the validation of the model is reported. It is an isolated street canyon with square buildings and aspect ratio W/H = 1, where W = 0.06 m is the width of the street and H = 0.06 m is the building height, corresponding to a physical scale model of 1:500 for the real street canyon case. The line source (width of 0.01 m) is located at ground level in the street centre. The 2D computational domain used in the simulations is evidenced in Fig. 1 by the bold line.

Boundary Conditions for the Model Validation Case

Details about boundary conditions employed in the simulations are available in Fig. 1. Different approaching maximum wind velocity values have been considered in the simulations: 1 m/s, 3 m/s and 4 m/s. The corresponding Reynolds numbers, calculated on the basis of the canyon height (H) are equal to 4000, 12000 and 16000, respectively. The physical properties of the air are taken at 25°C and atmospheric pressure. On the exit and upper side of the domain, a pressure and horizontal symmetry boundary conditions are imposed, respectively. At the inlet, different values of the intermediate turbulence variable for different wind speed values are imposed.

Approaching horizontal velocity profiles is available in Meroney *et al.* (1996), while mean inlet intermediate turbulence variable values $\hat{v}$ are obtained from a separate simulation of the channel upstream the canyon, chosen of

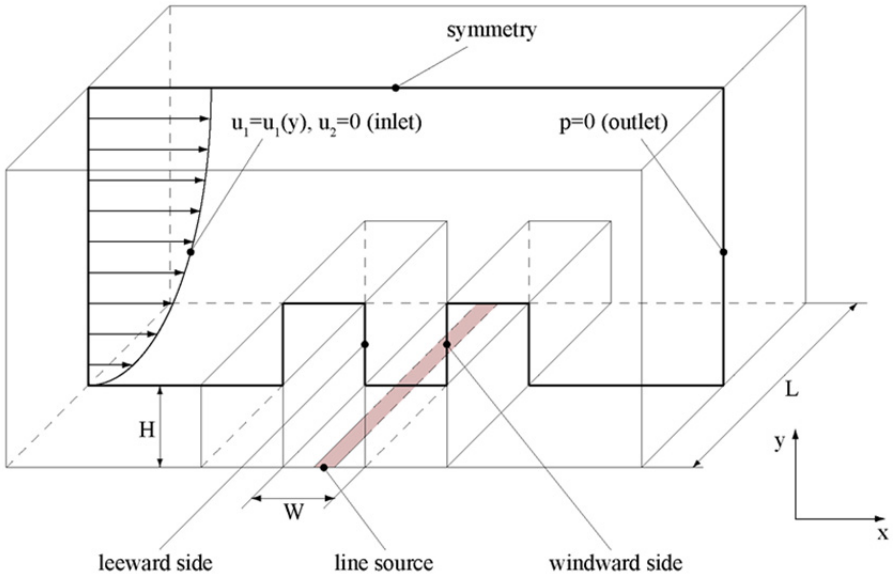

Fig. 1. Ethane dispersion simulation in an isolated street canyon: computational domain and boundary conditions employed.

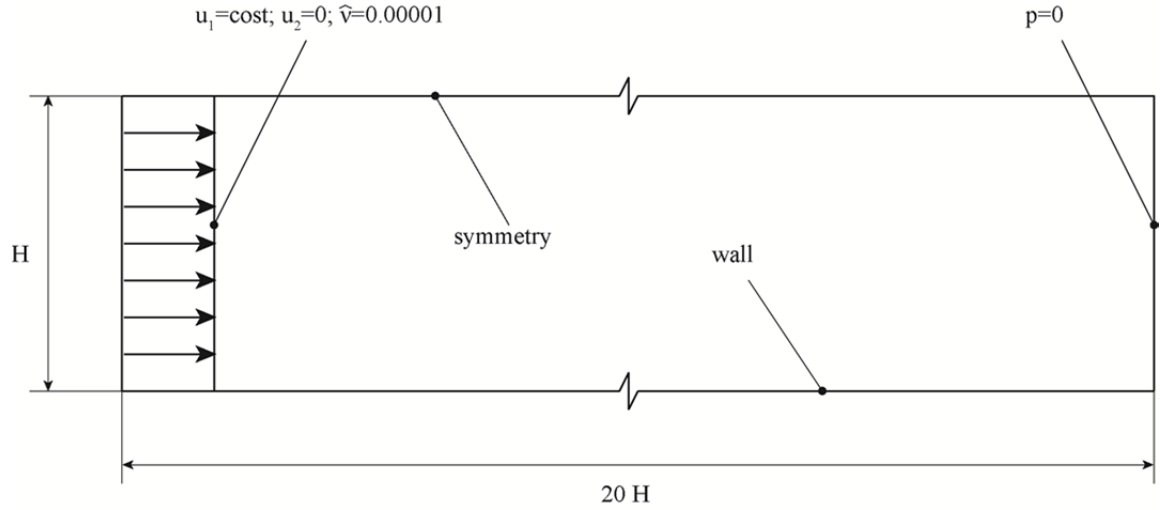

Fig. 2. Computational domain and boundary conditions considered for the evaluation of the mean turbulence intermediate variable $\hat{\nu}$ to be set at inlet section of the street canyon simulation.

appropriate length to allow the complete development of the flow. Details about the computational domain and the boundary conditions employed are available in Fig. 2. In particular, the upstream side of the canyon has been modelled as an horizontal channel with a constant inlet velocity profile and a symmetry boundary condition on the upper side. On the bottom side and at the channel exit, wall boundary condition and zero pressure boundary condition were imposed, respectively. At the inlet, a very low value of the intermediate turbulence variable was imposed ($\hat{\nu}$ = 0.0001), in accordance to prescriptions available in Saxena and Nair (2002). The mean value of the intermediate turbulence variable, and wind speed profile on the exit of the channel are used as inlet boundary conditions for the street canyon case. The simulations were performed for different wind speed velocity, corresponding to different mean values of the intermediate turbulence variable, as reported in Table 1.

As regards species conservation equation resolution, the following boundary conditions have been employed: zero concentration value has been set at the inlet section and at the top side of the domain; solid walls have been considered impermeable.

Emission Source for the Model Validation Case

The ethane source that represents pollutant from car exhausts, was modelled as a species flow rate that has been set equal to 4.54×10^{-5} mol/s. It corresponds to 4 L/h, as reported in experiments by Meroney *et al.* (1996), at atmospheric pressure and 25°C, assuming the ethane as an ideal gas. The diffusion coefficient of the ethane in air was assumed equal to 1.37×10^{-5} m^2/s at 25°C, estimated on the basis of the Chapman-Enskog theory (Chapman and Cowling, 1970).

Table 1. Value of the mean intermediate turbulence variable imposed at the SC inlet section for different approaching wind speeds, as obtained from numerical simulation of the wind tunnel tract upstream the SC.

Approaching wind speed (m/s)	Mean intermediate turbulence variable ($\hat{\nu}$)
1	0.00056
3	0.00261
4	0.00355
5	0.00445
10	0.00893
15	0.01337

Model Validation: Comparison with Experimental Data

The results of the ethane dispersion simulations are reported in terms of vertical profiles of concentration evaluated on leeward and windward sides of the canyon in correspondence of the building walls for three different values of the approaching wind speed (1 m/s, 3 m/s and 4 m/s). All the calculations were performed on computational grids obtained from a sensitivity analysis. The computational grid used is composed of about 20000 nodes and 39500 free triangular elements and are refined in correspondence of the solid walls in order to correctly capture the velocity boundary layer (Tominaga *et al.*, 2008). In Fig. 3 the comparison between the results obtained from the proposed numerical tool, and the experimental data are reported. In particular, the profiles in the figure show the dimensionless concentration K, expressed as a function of: real ethane concentration C (mol/m^3), reference wind speed u_{ref} (m/s), height of the building H (m), length of the line source L (m), and ethane flow rate Q_e (mol/s) through the following equation proposed by Meroney *et al.* (1996):

$$K = \frac{Cu_{ref}HL}{Q_e} \tag{10}$$

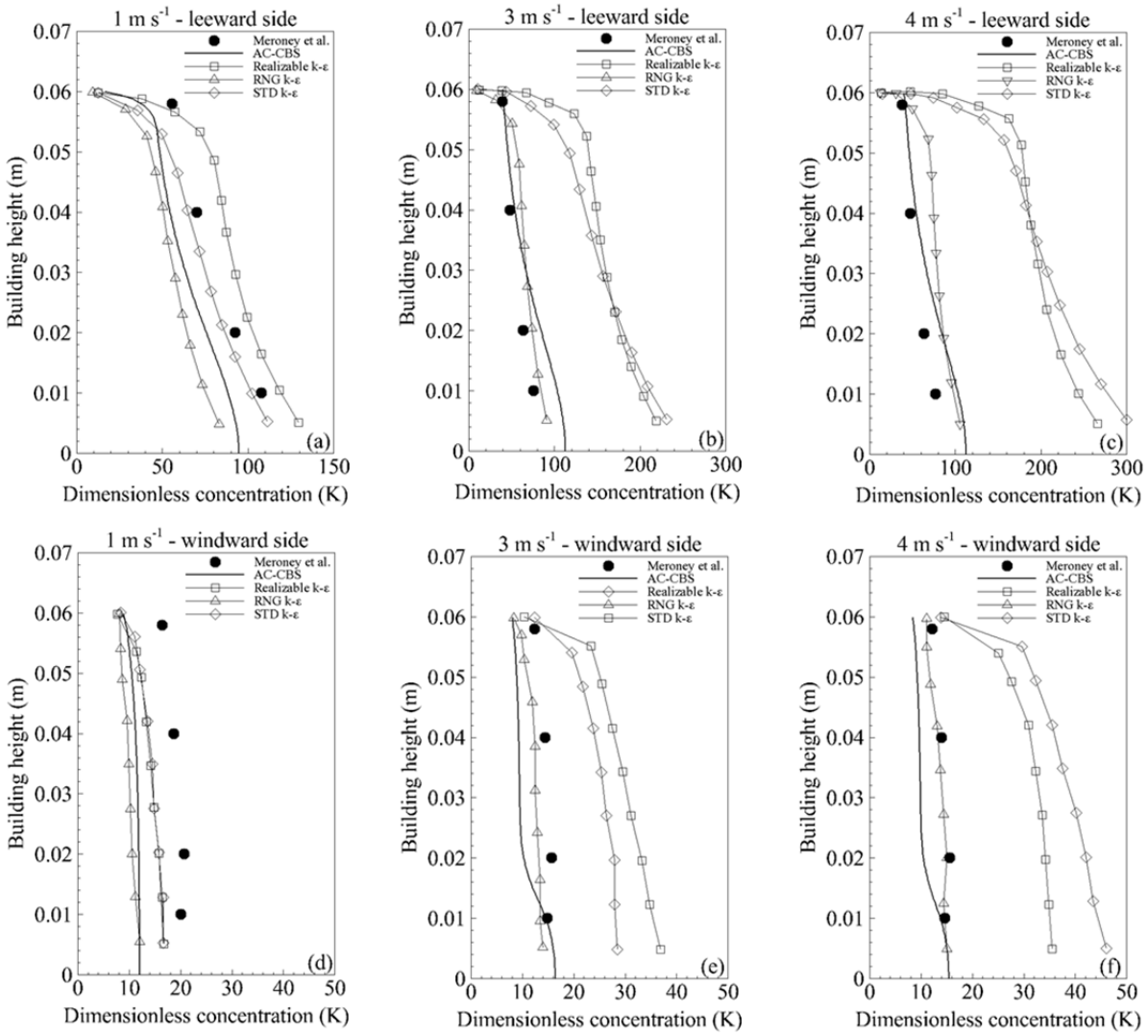

Fig. 3. Vertical profiles of dimensionless concentrations of ethane on leeward and windward sides of the isolated street canyon for different values of wind speed: comparison between the results obtained from the proposed model and the numerical and experimental data form the scientific literature (Chan *et al.*, 2002).

The Fig. 3 shows in general a good agreement of the numerical results from the proposed numerical model and the experimental data, with a better matching of the data for the highest value of wind speed both for leeward and windward sides of the canyon. In the windward side, the model tends to underestimate the experiments for all wind speed values; on the other hand, at the leeward side, the results from the present model underestimate ethane concentration for u = 1 m/s, while slightly overestimate experiments for the other wind velocity considered. On the leeward side, the concentration significantly decreases from the bottom of the street to the top of the upstream building; on the windward side however, the concentration variation as a function of the building height is generally less pronounced, even though in the case of u = 3 m/s and u = 4 m/s the obtained profiles show a slope change at the base of the canyon. The deviations of numerical results from experiments observed at low wind speed are expected to be related to the experimental uncertainties affecting the wind tunnel measurements, as evidenced by Meroney *et al.* (1996). In fact, the same data discrepancy was found also by Chan *et al*. (2002).

In the Fig. 3, the numerical results obtained from the proposed model, are compared also with three versions of the widely used two equations *k-ε* turbulence model: realizable *k-ε*, RNG (Renormalization Group) *k-ε* (Yakhot and Orszag. 1986) and standard (STD) *k-ε*. All these model versions are implemented in the commercial FLUENT® software, and have been employed in the simulations performed by Chan *et al.* (2002): except for the RNG version of the *k-ε* model, the STD and realizable versions show a clear overestimation of the experimental data that increases as the wind velocity increases, both at leeward and windward sides of the canyon. The proposed SA model performs similarly to the RNG version of the *k-ε* model and is expected to be less computationally demanding, especially for complex 3D problems, and is also expected to be more general. In fact, looking at the scientific literature, it can be observed that the RNG model results are strongly dependent on the values of model constants (Speziale and Thangam, 1992), that need to be tuned as a function of the case under investigation.

From the analysis of the Fig. 3, it can be also noted that at both leeward and windward sides of the canyon, the mean concentration values obtained from the proposed model weakly depend on the approaching wind speed. This is in accordance with the results obtained by Meroney *et al.* (1996), who stated that in the H/W = 1 canyon configuration, the pollutant dispersion in terms of dimensionless concentration is almost independent on the Reynolds number.

Model Application: UFPs Dispersion in Street Canyons

The model was applied to the simulation of UFPs dispersion in a real street canyon, where a source at its centre was placed, in order to simulate pollutant emission from vehicles. In Fig. 4 are reported the computational domain and the boundary conditions employed. The aspect ratio H/W was set equal to 1, with height of building from street level H, and width of the street, W equal to 14 m. The length of the SC has been considered infinite and so a two-dimensional (2D) domain has been employed for numerical investigations. Five different values of the approaching wind speed were considered in the present study: 1 m/s, 3 m/s, 5 m/s, 10 m/s, and 15 m/s. A uniform velocity profile has been imposed at the inlet section of the computational domain. The air physical properties have been taken at 25°C and atmospheric pressure. The Reynolds number corresponding to imposed air velocity values, and calculated on the basis of the canyon height (H), ranges from 9×10^5 to 1.4×10^7.

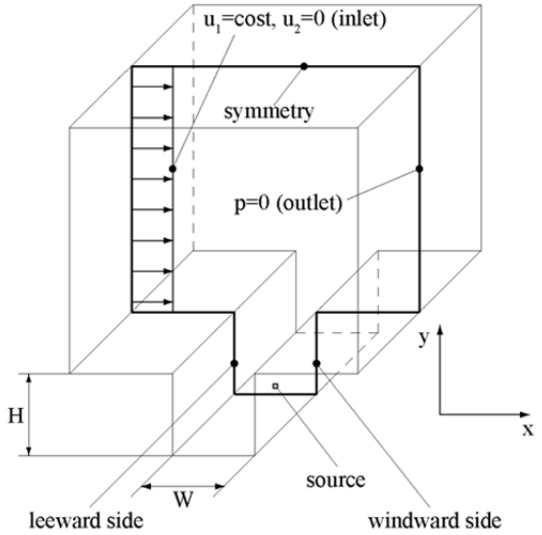

Fig. 4. Numerical modeling of UFPs concentration field in a real street canyon: computational domain and boundary conditions employed.

UFPs were modelled as a gas phase, imposing their diameter by the definition of a corresponding diffusion coefficient as reported by Baron and Willeke (2001). The relation between diffusion coefficient and UFPs diameter is:

$$D = \frac{kTC}{3\pi\eta d_p} \tag{11}$$

where D is the diffusion coefficient, k is the Boltzmann constant (1.38×10^{-23} Nm/K), C is a slip correction factor, η is the air viscosity and d_p the particle diameter. Since a particle size of 30 nm was considered as emitted by the source, the corresponding diffusion coefficient, calculated from equation (11) is $D = 6.2553 \times 10^{-9}$ m^2/s. Particles of 30 nm were considered since this is the typical mode of UFPs size distributions from vehicle combustion generated aerosols (Kittelson *et al.*, 2006; Wehner *et al.*, 2009).

UFPs concentration fields have been numerically obtained using different geometries, approaching wind speeds and source strength, in order to assess the influence of each parameter on the UFPs dispersion inside the canyon.

The size of the domain where UFPs source was imposed (a square with side length equal to 0.1 m, at 0.1 m from ground in the street centre) approximates the vehicle exhaust pipe size. This allows to reproduce the dilution effect of particles emitted from a road vehicle.

Parametric Analysis

In this paper, in order to evaluate the influential parameters on the UFPs exposure of pedestrians in urban microenvironment, a parametric analysis has been proposed. The reference approaching wind velocity has been set to 3 m/s in the analysis. The background concentration was set to 5.0×10^3 part./cm^3, kept constant for all the analysed cases. The reference UFPs source term was 1.01×10^7 part./cm^3/s, corresponding to the emission of Light Duty Vehicles (LDV) as reported from Keogh *et al.* (2010). With respect to the reference case, the parametric analysis was performed varying: i) the velocity of the approaching flow; ii) the geometry (aspect ratio *H/W*, step-up and step-down configuration) and iii) the emission source value. A summary of the parameters adopted in the performed parametric analysis is reported in Table 2.

As regards the traffic, the emission factors were evaluated on the basis of experimental data available in literature, as summarized in Table 3. The related source emission values were obtained considering a flux of about 17 vehicles/min.

Table 2. Influential parameters for the evaluation of geometry effect, traffic effect and wind speed effect on the dispersion of UFPs in a real SC.

Geometry	Traffic	Wind speed (m/s)
H/W = 1	Euro 6	1
H/W = 2	Fleet	3
H/W = 3	HDV	5
Step up	LDV-cruise	10
Step down	LDV-idle	15

RESULTS AND DISCUSSIONS

In this section, the results of UFPs dispersion simulations are reported. All the grids used in the simulations have been determined in the basis of a mesh sensitivity analysis. For simplicity, only the results about the sensitivity analysis performed for the square canyon (*H/W* = 1) are reported. Fig. 5 shows different grids used in the mesh sensitivity analysis composed by: (a) 8401; (b) 15048; (c) 28945; and (d) 60001 triangular elements. All the grids are refined in correspondence of the wall in order to properly capture the velocity boundary layer (Tominaga *et al.*, 2008).

Fig. 6 shows the vertical profiles of the horizontal component of the velocity at the leeward and windward sides of the canyon (at a distance of 1 m from the nearest wall) obtained from the four different grids employed. From the analysis of Fig. 6, it can be seen that no significant velocity variations have been obtained close to the street level, inside the canyon, when different computational grids are employed. On the basis of the obtained results, the mesh c has been chosen to perform the numerical analysis.

CFD Model Results: Flow Characteristics

The flow regimes in urban street canyons are determined by the interaction between the vortex generated behind the upwind building and the downwind building, and can be categorized in isolated roughness flow, wake interference flow and skimming flow (Oke, 1988; Hunter *et al.*, 1990). In the case of isolated roughness flow, because of the distance between the buildings, the interaction between the vortices formed on the downwind building and the upwind building is negligible. If the buildings are less distant, this interaction between the two vortices is possible, producing a wake interference flow. The skimming flow regime is usually characterized by the presence of a single main vortex inside the canyon (Baik and Kim, 1999). In two-dimensions, the height to width ratio strongly influences the flow field characteristic inside the canyon.

In Fig. 7, the streamlines obtained for the following different configurations of the canyon geometry is reported: *H/W* = 1 (Fig. 7(a)); *H/W* = 2 (Fig. 7(b)); *H/W* = 3 (Fig. 7(c)); and step down configuration (Fig. 7(d)). According with the flow definition of Oke (1988), in all the four cases analysed, a skimming flow regime was found. From the figure it can be observed that in the *H/W* = 1 case there is only one main single clockwise rotating vortex and two small secondary vortices on the two corner bases of the canyon, as described by Baik and Kim (1999) and Hassan and Crowther (1998), with the centre of the main vortex located approximately at the centre of the canyon. In the *H/W* = 2 case, in which the building height is double of the street width, there are two main vortices rotating in opposite direction: the upper vortex rotating clockwise, and the lower vortex rotating counter clockwise: this agrees with the findings of Hunter *et al.* (1992) and Sini *et al.* (1996) who found the same two-vortex configuration, but contrasts with the studies of (Johnson and Hunter, 1999), where a single vortex was observed. The two secondary vortices at corner base of the canyon are still present but result weaker. Since the grid independency has been ensured by a proper mesh sensitivity analysis, the size reduction of secondary vortices is probably due to the reduced velocity of the main lower vortex with respect to the square cavity case. In the *H/W* = 3 case (the building height is threefold the street width) three main vortex were recognized. The upper one, as in the *H/W* = 1 and *H/W* = 2 cases, rotates clockwise because of the direction of the above free stream; the middle and lower vortices are counter clockwise and clockwise rotating, respectively, in

Table 3. Different emission factors and UFPs source terms as a function of traffic type.

Traffic type	Emission factor (part./km/veh)	Source value (part./m^3/s)
Euro 6	6.00×10^{11} (Commission Regulation (EC) No 692/2008)	1.67×10^{10}
Fleet	7.26×10^{14} (Keogh *et al.*, 2010)	2.02×10^{13}
HDV	6.40×10^{15} (Keogh *et al.*, 2010)	6.11×10^{13}
LDV-cruise	3.63×10^{14} (Keogh *et al.*, 2010)	1.01×10^{13}
LDV-idle	4.67×10^{13} (Jayaratne *et al.*, 2009; Keogh *et al.*, 2010)	1.30×10^{12}

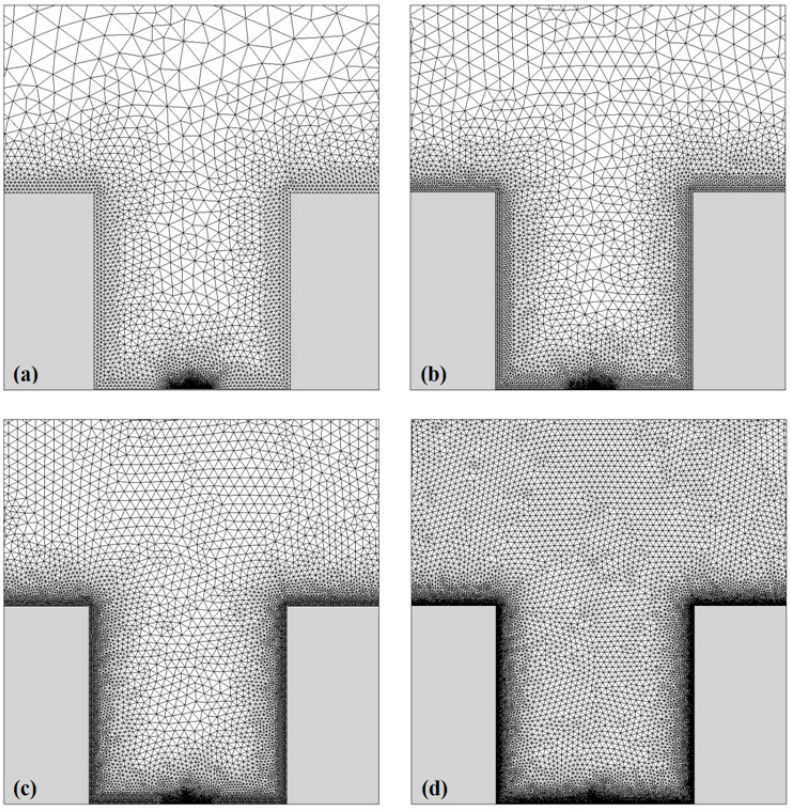

Fig. 5. Numerical simulation of a real square SC. Computational grids considered to perform grid sensitivity analysis composed by: (a) 8401; (b) 15048; (c) 28945; and (d) 60001 triangular elements.

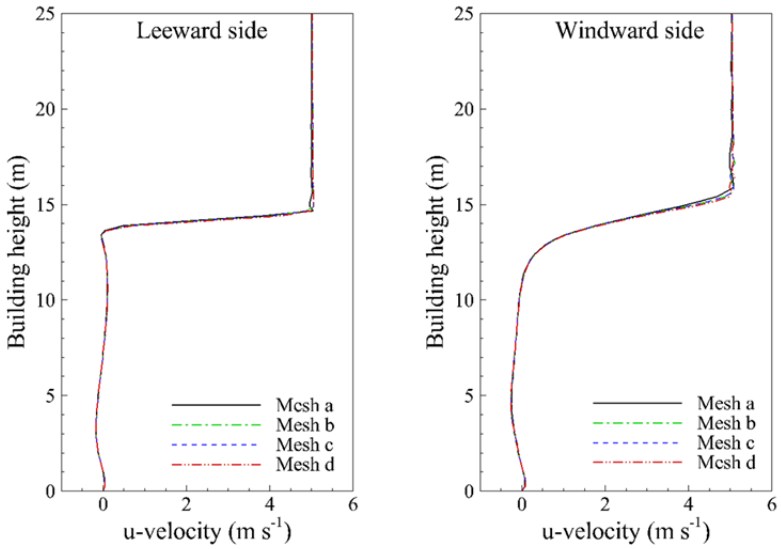

Fig. 6. Numerical simulation of a real SC: vertical profiles of the horizontal component of the velocity on the leeward and windward sides of the SC, at a distance of 1 m from the nearest wall, obtained employing the four computational grids available in Fig. 5 Approaching wind velocity set to 3 m/s.

accordance with Sini *et al.* (1996), who stated that in very narrow street case, a multi vortex skimming flow regime can be found. In the H/W = 3 configuration, the two secondary vortices at the bottom corners are almost disappeared. In fact, as the H/W ratio increases, the energy transferred from the free stream region to the two secondary vortices at corner base decreases. Halving the downstream building height, the step down configuration is achieved. In this case there are two main vortices rotating in opposite direction but they appear stretched in respect of the symmetric canyon configuration: the upper clockwise rotating vortex results extended and covers the downwind building roof, the lower

vortex results flattened.

Fig. 8 shows turbulent intermediate variable $\hat{v}$ (Fig. 8(a)), vorticity (Fig. 8(b)) and Reynolds stress (Fig. 8(c)) distributions inside the H/W = 1 street canyon geometry. The intermediate turbulent variable significantly increases at the centre and at the top side of the canyon. As a consequence, momentum and species diffusion increases: enhancing momentum transfer from the free stream region to the flow region inside the canyon; facilitating UFPs dispersion from the canyon to the free stream region. From the analysis of Fig. 8(c), the Reynolds stress shows different zones with positive and negative values. In the upper region of the canyon, the model predicts negative Reynolds stress, with a peak on the windward side. Following the definition of Raupach (1981), this zone may be originated by the sweeps, which are a contribution to the mean Reynolds stress originated by a situation whereby $u'_i \geq 0$ and $u'_j \leq 0$. Rotach (1993) used the method of conditional sampling in order to investigate the nature and mechanisms of turbulent processes and concluded that sweeps were associated with large scale motions and that momentum is transported inside the canyon by eddies penetrating from above. From Fig. 8(c), it can be observed that these sweeps predominantly occur on the windward side of the canyon. Following the same definition of Raupach (1981), the zones in which the Reynolds stress is predicted to be positive correspond to outward interaction ($u'_i \geq 0$ and $u'_j \geq 0$) or inward interaction ($u'_i \leq 0$ and $u'_j \leq 0$). According to Baik and Kim (2002), since the mean flow at roof level is horizontal, turbulent processes are responsible of the transport of pollutants outside the canyon through the turbulent diffusion.

CFD Model Results: Parametric Analysis on Concentration Profiles

The dependence of UFPs dispersion on the street canyon configuration, wind speed and pollutant source type, is evidenced in Fig. 9, that shows the vertical concentration profiles of UFPs calculated on leeward and windward

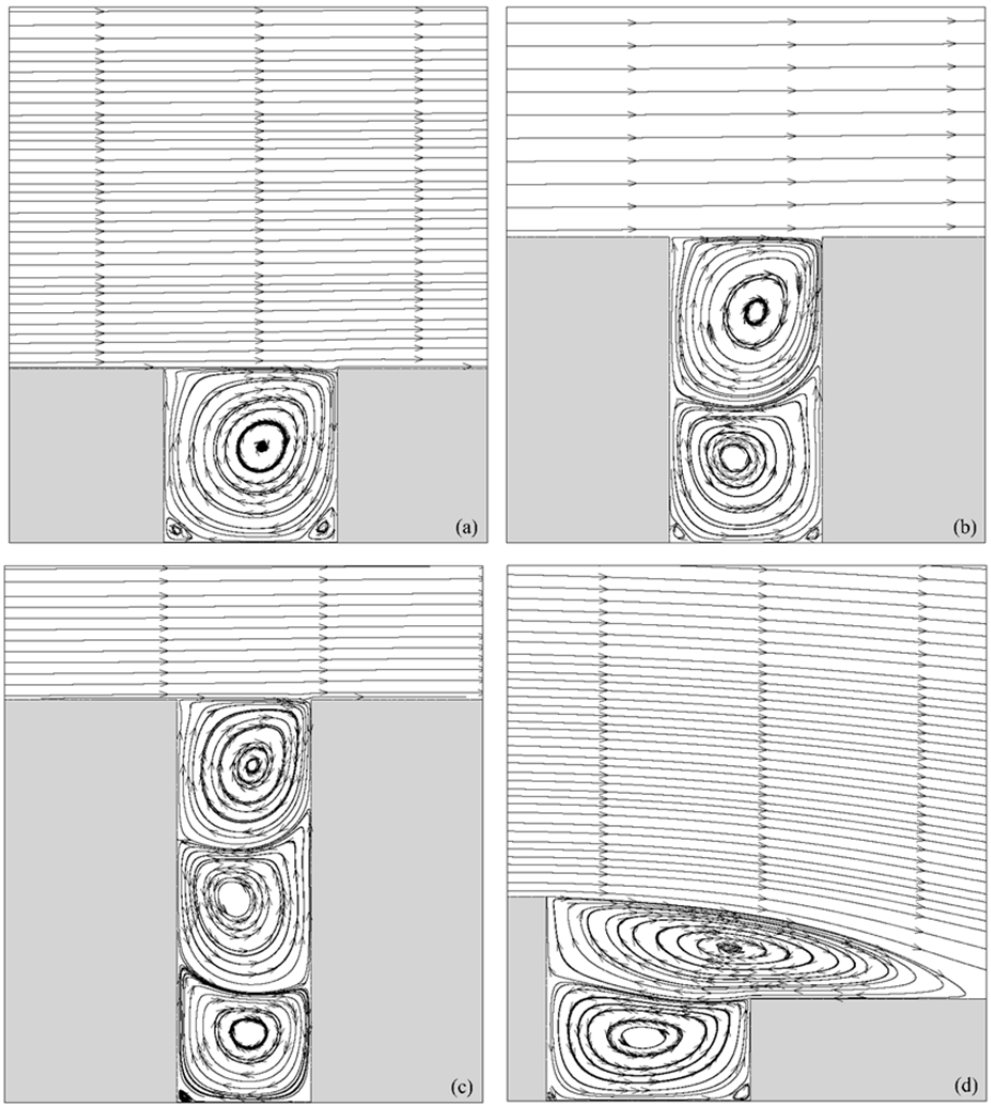

Fig. 7. Numerical simulation of a real SC. Streamlines obtained for different geometrical configurations: (a) H/W = 1; (b) H/W = 2; (c) H/W = 3; (d) step down configuration. Approaching wind velocity set to 3 m/s.

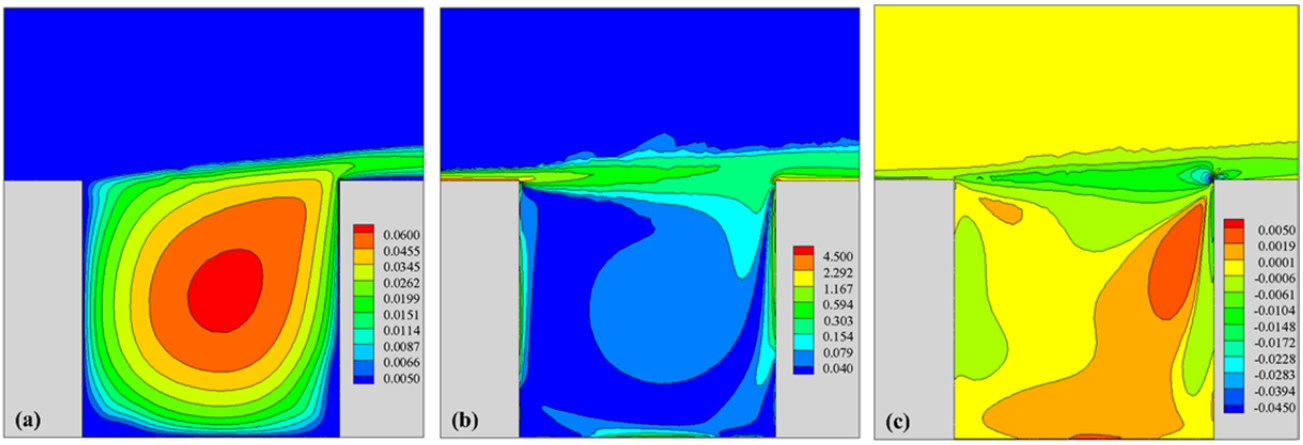

Fig. 8. Numerical simulation of a real square SC: (a) field of intermediate turbulence variable $\hat{\nu}$; (b) vorticity distribution; and (c) Reynolds stress distribution normalized with respect to the reference wind speed of 3 m/s.

sides of the canyon at a distance of 1 m from the nearest building walls, corresponding to the sidewalks zones, as geometry, wind speed and traffic type vary.

Geometry Effect

The effect of the building height on the UFPs dispersion is shown in Fig. 9(a). The traffic considered is the LDV (source equal to 1.01×10^7 part./cm^3/s) and the wind speed is 3 m/s. As the building height increases (i.e., the *H/W* aspect ratio), the mean value of the concentration becomes higher. Higher concentrations were detected on leeward or windward sides according to the number and the direction of rotation of mean vortices; i.e. the aspect ratio: in the *H/W* = 1 configuration, UFPs concentration values results higher on the leeward side; whereas, in the *H/W* = 2 configuration the concentration is higher on the windward side. Furthermore, the Fig. 9(a) shows a significant increase of the concentration for the *H/W* = 3 configuration, because the interaction between the roof wind and street level wind becomes weaker, leading to a more intense stagnant phenomena in the canyon.

Fig. 9(b) shows the influence of the step down configuration compared to the symmetric street canyon: in the step down configuration, the concentration becomes higher on the windward side and the vertical profile shows a strong decrease at about 6 m from the ground due to the halving of the downwind building.

Wind Speed Effect

The increase of wind speed enhances the air exchange from the canyon to the above undisturbed flow, resulting in a reduced concentration of particles (Buonanno *et al.*, 2011). The Fig. 9(c) quantifies the wind speed effect on particle concentration for different wind speed values: when the wind speed decreases, the concentration vertical profiles shift to higher values. Therefore, on the windward side, the vertical concentration remains almost constant, whilst, on the leeward side, it decreases exponentially in the first 5 m from the ground; this behaviour is significantly noticeable for the lowest wind speed value (1 m/s), indicating the formation of an accumulation zone in the lower corner of the leeward wall. With higher values of wind speed, the increased ventilation enhances the dispersion of particles, then, the profiles on leeward side become almost constant; moreover, also the difference of concentration between leeward and windward side tends to decrease.

Traffic Effect

The Fig. 9(d) shows the effect of different kinds of traffic on the UFPs dispersion. The analysis was performed for an aspect ratio *H/W* = 1, the approaching wind speed was equal to 3 m/s, with a constant background concentration value of 5.0×10^3 part./cm^3. Different traffic types lead to different emission factor values, as reported in

Table **3**. As the source strength increases (from LDV, to fleet, and HDV), an higher value of the mean concentration can be observed. In particular, the UFPs concentration results higher in correspondence of the leeward side for all the considered traffic types; besides, the difference between UFPs concentration at leeward and windward side increases in correspondence of the highest values of the emission source (HDV traffic type).

CFD Model Results: Assessment of Pedestrian Exposure to UFPs in a Real SC.

In this section, an assessment of pedestrians exposure UFPs in a real SC is reported, as a function of SC aspect ratio and configuration, pedestrian position at the street level (leeward, centre or windward side), and wind velocity. On the basis of the simulation results reported in section 3.2, UFPs concentration values in 3 points of the domain are reported as a function of the different parameters analysed. The three points considered in the domain simulate the position of the pedestrians, and are located on leeward and windward sides at a height of 1.5 m, at 2 m from the nearest walls, and at the centre of the street at the same height (1.5 m). Fig. 10 shows the UFPs concentration as a function of: i) aspect ratio, ii) traffic type, iii) wind velocity, iv) step up and step down configurations.

The exposure of pedestrian generally increases as the aspect ratio increases and results larger on leeward or windward side alternatively (Fig. 10(a)); the highest exposure value is related to the emission of HDV on the leeward

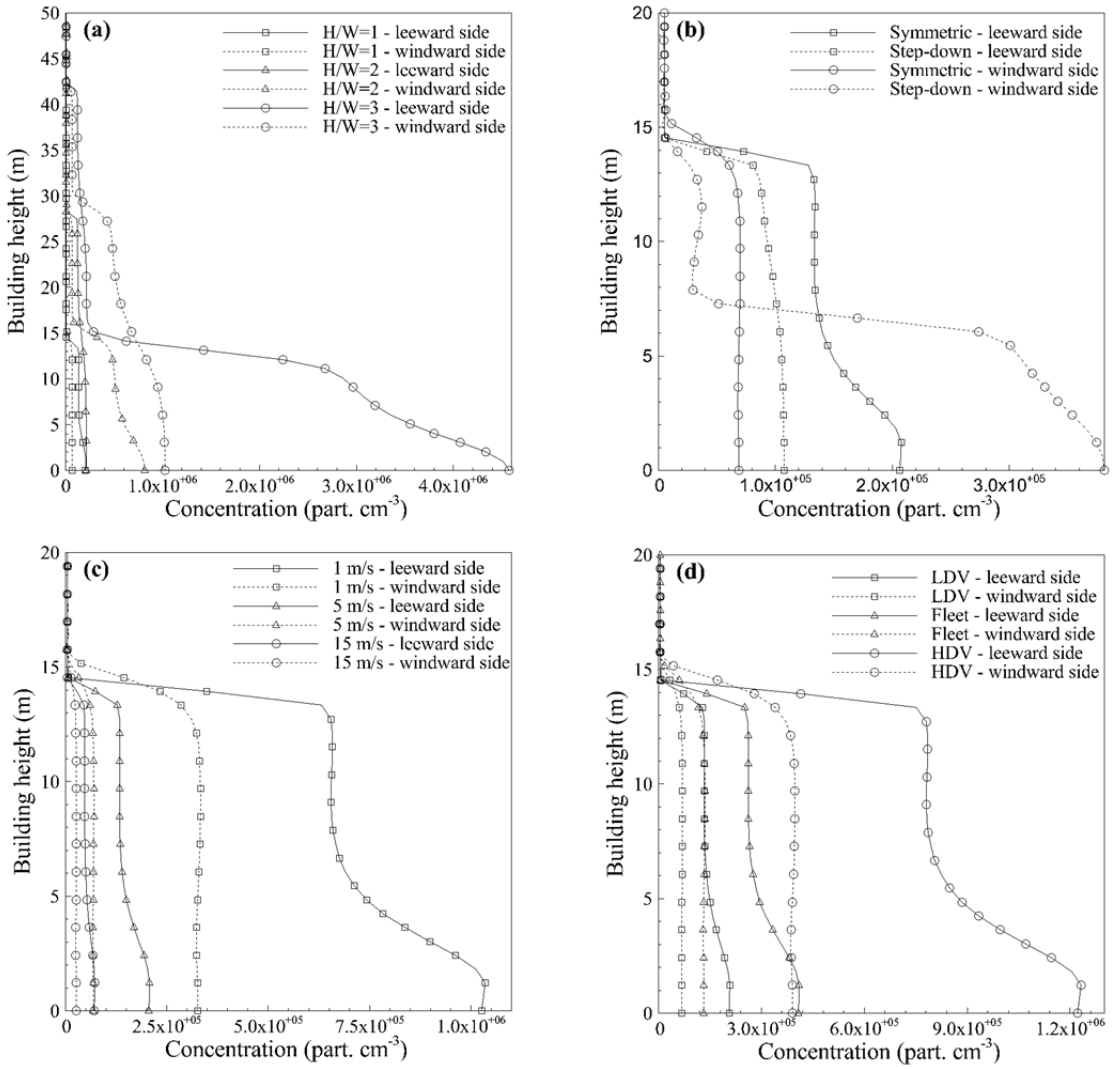

Fig. 9. Numerical simulation of a real SC: vertical profiles of UFPs concentration as function of geometry, wind speed and traffic types, obtained on the leeward and windward sides of the SC, at a distance of 1 m from the nearest wall.

side, while the lowest ones are referred to the emission of Euro 6 vehicles (Fig. 10(b)), with UFPs concentration equal to approximately the background value (≈ 5000 part./cm^3). With the increasing of wind speed, a decreasing of the concentration on both leeward and windward sides as well as on the centre of the street is observed. Fig. 10(c) evidences that at low wind speed condition, even a small increase of such parameter causes a significant reduction of UFPs concentration in all the investigated points into the SC. The dependence of pedestrians exposure to UFPs becomes weak when the wind velocity is larger than 5 m/s.

CONCLUSIONS

In this paper, numerical investigations about UFPs dispersion in street canyons were performed by employing a non-commercial numerical tool based on the Artificial Compressibility (AC) version of the Characteristic Based Split (CBS) algorithm, the one equation Spalart-Allmaras (SA) turbulence model and a *K*-theory species transport equation for the calculation of UFPs concentration. In the author's knowledge, the SA turbulence model has been applied for the first time to the simulation of turbulent flow in a SC, performing similar to the RNG version of thewidely used *k*-*ε* turbulence model. The interest in the SA turbulence model is related to the possibility to switch to Detached Eddy Simulation (DES) and to the reduced computational cost when complex three-dimensional problems are investigated. The numerical algorithm was stabilized by employing an order of magnitude analysis of each term of the governing equations, obtaining a stable and robust procedure. The proposed numerical scheme has been validated against experiments of ethane dispersion in a wind tunnel model of street canyon, available in the scientific literature. The profiles of dimensionless ethane concentration obtained from the simulations for different approaching wind velocities, were compared to experiments showing a very good agreement. The validated scheme was applied to the simulation of UFPs dispersion in a real street canyon, evaluating the influence of parameters such

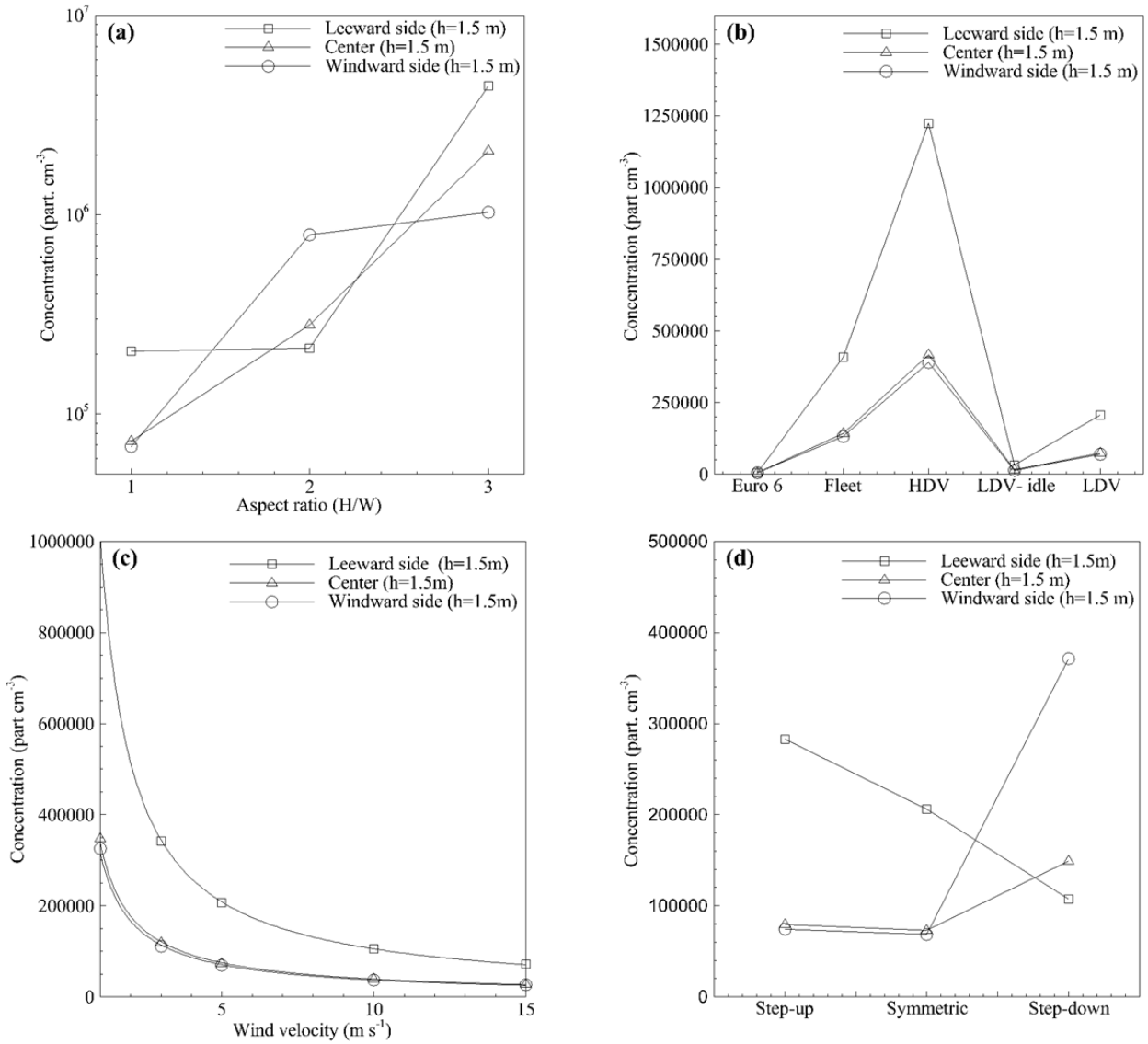

Fig. 10. Numerical simulation of a real SC: pedestrian exposure to UFPs as a function of geometry, wind speed and traffic, evaluated at leeward and windward sides, at a height of 1.5 m and in different positions at the street level.

as the geometry of the street, wind speed, and the traffic type on the exposure of pedestrians to UFPs. The obtained results showed that with the increasing of the street canyon aspect ratio *H/W*, that is the ratio between building height and buildings distance, the dispersion of particles in the canyon becomes weaker due to the formation of different vortices that reduce vertical air exchange with the above roof-level atmosphere. The maximum UFPs concentration value (5.0×10^6 part./cm^3) was found on the leeward side of the canyon in the case of *H/W* = 3 configuration and for a wind speed of 5 m/s. As concerns the wind speed, it was found that even though a higher value of the approaching flow facilitates the dispersion of the particles, this effect becomes weak when the wind speed is larger than 5 m/s. The traffic effect has been evaluated by imposing different UFPs source values as a function of the vehicles type, obtaining, as expected, the lowest UFPs concentration when Euro 6 vehicles are considered. In this case, the maximum calculated concentration value was found to be of the same order of magnitude of the background concentration value (5.0×10^3 part./cm^3). On the contrary, the highest UFPs concentration was found on the leeward side when High Duty Vehicles (1.2×10^6 part./cm^3) were considered in the simulations. UFPs concentration dependence on the SC configuration has also been numerically investigated analysing the step up and step down cases, and showing that pedestrian exposure to UFPs increases at the leeward side when the step up case is considered, and at the windward side in the step down configuration.

REFERENCES

Andersen, Z.J., Wahlin, P., Raaschou-Nielsen, O., Ketzel, M., Scheike, T. and Loft, S. (2008). Size Distribution and Total Number Concentration of Ultrafine and Accumulation Mode Particles and Hospital Admissions

in Children and Elderly in Copenhagen. *Occup. Environ. Med.* 65: 458–466.

Andersen, Z.J., Olsen, T.S., Andersen, K.K., Loft, S., Ketzel, M. and Raaschou-Nielsen, O. (2010). Association between Short-Term Exposure to Ultrafine Particles and Hospital Admissions for Stroke in Copenhagen, Denmark. *Eur. Heart J.* 16: 2034–2040.

Arpino, F., Carotenuto, A., Massarotti, N. and Nithiarasu, P. (2008). A Robust Model and Numerical Approach for Solving Solid Oxide Fuel Cell (SOFC) Problems. *Int. J. Numer. Methods Heat Fluid Flow* 18: 811–834.

Arpino, F., Massarotti, N., Mauro, A. and Nithiarasu, P. (2009). Artificial Compressibility-Based CBS Scheme for the Solution of the Generalized Porous Medium Model. *Numer. Heat Transfer, Part B* 55: 196–218.

Arpino, F., Massarotti, N. and Mauro, A. (2010). High Rayleigh Number Laminar-Free Convection in Cavities: New Benchmark Solutions. *Numer. Heat Transfer, Part B* 58: 73–97.

Arpino, F., Massarotti, N. and Mauro, A. (2010). A Stable Explicit Fractional Step Procedure for the Solution of Heat and Fluid Flow through Interfaces between Saturated Porous Media and Free Fluids in Presence of High Source Terms. *Int. J. Numer. Methods Eng.* 83: 671–692.

Arpino, F., Buonanno, G., Scungio, M., Massarotti, N. and Mauro, A. (2011). A Roboust Artificial Compressibility Algorithm for Turbulent Incompressible Flows in Urban Areas, Second International Conference on Computational Methods for Thermal Problems, Dalian, China.

Arpino, F., Massarotti, N. and Mauro, A. (2011). Efficient Three-Dimensional FEM Based Algorithm for the Solution of Convection in Partly Porous Domains. *Int. J. Heat Mass Transfer* 54: 4495–4506.

Commission Regulation (EC) No 692/2008. Commission Regulation (EC) No 692/2008 of 18 July 2008 implementing and amending Regulation (EC) No 715/2007 of the European Parliament and of the Council on Type-Approval of Motor Vehicles with Respect to Emissions from Light Passenger and Commercial Vehicles (Euro 5 and Euro 6) and on Access to Vehicle Repair and Maintenance Information.

Council Directive 1999/30/EC Council Directive 1999/30/EC of 22 April 1999 Relating to Limit Values for Sulphur Dioxide, Nitrogen Dioxide and Oxides of Nitrogen, Particulate Matter and Lead in Ambient Air. L 163, Official Journal of the European Union.

D'Acunto, B. (2004). *Computational Methods for PDE in Mechanics*, Series on Advances in Mathematics for Applied Sciences 67, World Scientific Publishing Co Pte Ltd., Singapore.

Directive 2008/50/EC. Directive 2008/50/EC of The European Parliament and of The Council of 21 May 2008 on Ambient Air Quality and Cleaner Air for Europe. L 152/1, Official Journal of the European Union.

Eiguren-Fernandez, A., Shinyashiki, M., Schmitz, D.A., DiStefano, E., Hinds, W., Kumagai, Y., Cho, A.K. and Froines, J.R. (2010). Redox and Electrophilic Properties of Vapor- and Particle-Phase Components of Ambient Aerosols. *Environ. Res.* 10: 207–212.

Gidhagen, L., Johansson, C., Langner, J. and Foltescu, V.L. (2005). Urban scale Modelling of Particle Number Concentration in Stockholm. *Atmos. Environ.* 39: 1711–1725.

Hassan, A.A. and Crowther, J.M. (1998). Modelling of Fluid Flow and Pollutant Dispersion in a Street Canyon. *Environ. Monit. Assess.* 52: 281–297.

Hasse, C., Sohm, V. and Durst, B. (2009). Detached Eddy Simulation of Cyclic Large Scale Fluctuations in a Simplifiedengine Setup. *Int. J. Heat Fluid Flow* 30: 32–43.

Hirsch, C. (2007). *Numerical Computation of Internal and External Flows*, Fundamentals of Computational Fluid Dynamics 1, John Wiley & Sons, Inc. New York, USA.

Holmes, N.S. and Morawska, L. (2006). A Review of Dispersion Modelling and Its Application to the Dispersion of Particles: An Overview of Different Dispersion Models Available. *Atmos. Environ.* 40: 5902–5928.

Hunter, L.J., Johnson, G.T. and Watson, I.D. (1992). An Investigation of Three Dimensional Characteristics of Floe Regimes within the Urban Canyon. *Atmos. Environ.* 26B: 425–432.

Hunter, L.J., Watson, I.D. and Johnson, Y.E (1990). Modelling Air Flow Regimes in Urban Canyons. *Energ. Buildings* 15: 315–324.

Jayaratne, E.R., Wang, L. Heuff, D., Morawska, L. and Ferreira, L. (2009). Increase in Particle Number Emissions from Motor Vehicles due to Interruption of Steady Traffic Flow. *Transp. Res. Part D: Transport Environ.* 14: 521–526.

Johnson, J.T. and Hunter, L.J. (1999). Some Insights into Typical Urban Canyon Airflows. *Atmos. Environ.* 33: 3991–3999.

Keogh, D.U., Kelly, J., Mengersen, K., Jayaratne, R., Ferreira, L. and Morawska, L. (2010). Derivation of Motor Vehicle Tailpipe Particle Emission Factors Suitable for Modelling Urban Fleet Emissions and Air Quality Assessments. *Environ. Sci. Pollut. Res. Int.* 17: 724–739.

Ketzel, M. and Berkowicz, R. (2004). Modelling the Fate of Ultrafine Particles from Exhaust Pipe to Rural Background: an Analysis of Time Scales for Dilution, coagulation and deposition. *Atmos. Environ.* 38: 2639–2652.

Kim, J.J. and Baik, J.J. (2001). Urban Street-Canyon Flows with Bottom Heating. *Atmos. Environ.* 35: 3395–3404.

Kim, K.J. and Baik, J.J. (2004). A Numerical Study of the Effects of Ambient wind Direction on Flow and Dispersion in Urban Street Canyons Using the RNG k-ε Turbulence Model. *Atmos. Environ.* 38: 3093–3048.

Kittelson, D.B., Watts, W.F. and Johnson, J.P. (2004). Nanoparticle Emissions on Minnesota Highways. *Atmos. Environ.* 38: 9–19.

Kittelson, D.B., Schauer, J.J., Lawson, D.R., Watts, W.F. and Johnson, J.P. (2006). On-Road and Laboratory Evaluation of Combustion Aerosols - Part 2: Summary of Spark Ignition Engine Results. *J. Aerosol Sci.* 37: 931–949.

Launder, B. and Spalding, D. (1974). The Numerical Computation of Turbulent Flows. *Comput. Meth. Appl. Mech. Eng.* 3: 269–289.

Letzel, M.O., Krane, M. and Raasch, S. (2008). High Resolution Urban Large-Eddy Simulation Studies from Street Canyon to Neighbourhood Scale. *Atmos. Environ.* 42: 8770–9784.

Li, X.X., Liu,C.H., Leung, D.Y.C. and Lam, K.M. (2006). Recent Progress in CFD Modelling of wind Field and Pollutant Transport in Street Canyons. *Atmos. Environ.* 40: 5640–5658.

Liu, C.H., Barth, M.C. and Leung, D.Y.C. (2004). Large-Eddy Simulation of Flowand Pollutant Transport in Street canyons of Different Building-Height-to-Street-Width Ratios. *J. Appl. Meteorol.* 43: 1410–1424.

Liu, C.H., Leung, D.Y.C. and Barth, M.C. (2005). On the Prediction of Air and Pollutant Exchange Rates in Street Canyons of Different Aspect Ratios Using Large-Eddy Simulation. *Atmos. Environ.* 39: 1567–1574.

Massarotti, N., Arpino, F., Lewis, R.W. and Nithiarasu, P (2006). Explicit and Semi-Implicit CBS Procedures for Incompressible Viscous Flows. *Int. J. Numer. Methods Eng.* 66: 1618–1640.

Meroney, R.N., Pavageau, M., Rafailidis, S. and Schatzmann, M. (1996). Study of Line Source Characteristics for 2-D Physical Modelling of Pollutant Dispersion in Street Canyons. *J. Wind Eng. Ind. Aerodyn.* 62: 37–56.

Møller, P., Folkmann, J.K., Forchhammer, L., Bräuner, E.V., Danielsen, P.H., Risom, L. and Loft, S. (2008). Air Pollution, Oxidative Damage to DNA, and Carcinogenesis. *Cancer Lett.* 266: 84–97.

Moreira, D. and Vilhena, M. (2010). *Air Pollution and Turbulence: Modeling and Applications*, CRC Press/ Taylor & Francis, United States.

Nel, A., Xia, T., Mädler, L. and Li, N. (2006). Toxic Potential of Materials at the Nanolevel. *Science* 311: 622–627.

Oke, T.R. (1988). Street Design and Urban Canopy Layer Climate. *Energ. Buildings* 11: 103–113.

Paik, J., Sotiropoulos, F. and Porté-Agel, F. (2009). Detached Eddy Simulation of Flow around Two Wall-Mounted Cubes in Tandem. *Int. J. Heat Fluid Flow* 30: 286–305.

Pohjola, M., Pirjola, L. Kukkonen, J. and Kulmala, M. (2003). Modelling of the Influence of Aerosol Processes for the Dispersion of Vehicular Exhaust Plumes in Street Environment. *Atmos. Environ.* 37: 339–351.

Pope, C.A. and Dockery, D.W. (2006). Health Effects of Fine Particulate Air Pollution: Lines that Connect. *J. Air Waste Manage. Assoc.* 56: 709–742.

Pope III, C.A. and Dockery, D.W. (2006). Health Effects of Fine Particulate Air Pollution: Lines That Connect. *J. Air Waste Manage. Assoc.* 56: 707–742.

Raupach, M.R. (1981). Conditional Statistics of Reynolds Stress in Rough-Wall and Smooth-Wall Turbulent Boundary Layers. *J. Fluid Mech.* 108: 363–382.

Rotach, M.W. (1993). Turbulence Close to a Rough Urban Surface Part I: Reynolds Stress. *Boundary Layer Meteorol.* 65: 1–28.

Saxena, S.K. and Nair, M.T. (2002). Implementation and Testing of Spalart-Allmaras Model in a Multi-Block Code, 40th AIAA Aerospace Sciences Meeting and Exhibit, January 14–27, 2002, Reno, NV.

Sharma, P. and Khare, M. (2001). Modelling of Vehicular Exhausts-a Review. *Transp. Res. Part D: Transport Environ.* 6: 179–198.

Sini, J.F., Anquetin, S. and Mestayer, P.G. (1996). Pollutant Dispersion and Thermal Effects in Urban Street Canyon. *Atmos. Environ.* 30: 2659–2677.

Spalart, P.R. and Allmaras, S.R. (1992). A One Equation Turbulence Model for Aerodynamic Flows. *AIAA Paper* 92–0439.

Speziale, C.G. and Thangam, S. (1992). Analysis of an RNG Based Turbulence Model for Separated Flows. *Int. J. Eng. Sci.* 30: 1379–1388.

Tominaga, Y., Mochida, A., Yoshie, R., Kataoka, H., Nozu, T., Yoshikawa, M. and Shirasawa, T. (2008). AIJ Guidelines for Practical Applications of CFD to Pedestrian Wind Environment around Buildings. *J. Wind Eng. Ind. Aerodyn.* 96: 1749–1761.

Tominaga, Y. and Stathopoulos, T. (2011). CFD Modeling of Pollution Dispersion in a Street Canyon: Comparison between LES and RANS. *J. Wind Eng. Ind. Aerodyn.* 99: 340–348.

Vardoulakis, S., Fisher, B.R.A., Pericleous, K. and Gonzalez-Flesca, N. (2003). Modelling Air Quality in Street Canyons: A Review. *Atmos. Environ.* 37: 155–182.

Venetsanos, A., Bartzis, J., Wurtz, J. and Papailiou, D.D. (2003). Comparative Modeling of a Passive Release from an l-Shaped Building Using One, Two and Three-Dimensional Dispersion Models. *Int. J. Environ. Pollut.* 3: 129–143.

Vignati, E., Berkowicz, R., Palmgren, F., Lyck, E. and Hummelshoj, P. (1999). Transformation of Size Distributions of Emitted Particles in Streets. *Sci. Total Environ.* 235: 37–49.

Viswanathan, A.K. and Tafti, D.K. (2006). Detached Eddy Simulation of Flow and Heat Transfer in Fully Developed Rotating Internal Cooling Channel with Normal Ribs. *Int. J. Heat Fluid Flow* 27: 351–370.

Walton, A. and Cheng, A.Y.S. (2002). Large-Eddy Simulation of Pollution Dispersion in an Urban Street Canyon - Part II: Idealised Canyon Simulation. *Atmos. Environ.* 36: 3615–3627.

Wehner, B., Uhrner, U., von Löwis, S., Zallinger, M. and Wiedensohler, A. (2009). Aerosol Number Size Distributions within the Exhaust Plume of a Diesel and a Gasoline Passenger Car Under on-Road Conditions and Determination of Emission Factors. *Atmos. Environ.* 43: 1235–1245.

Xie, X., Huang, Z. and Wang, J.S. (2005). Impact of Building Configuration on Air Quality in Street Canyon. *Atmos. Environ.* 39: 4519–4530.

Yakhot, V. and Orszag, S.A. (1986). Renormalization Group Analysis of Turbulence: I. Basic Theory. *J. Sci. Comput.* 1: 1–51.

Zienkiewicz, O.C., Taylor, R.L. and Nithiarasu, P. (2005). *The Finite Element Method for Fluid Dynamics*, Butterworth and Heinemann, Amsterdam, Boston, USA.

Received for review, November 6, 2012
Accepted, April 25, 2013